Cancer Cell
Article

Yes and PI3K Bind CD95 to Signal Invasion of Glioblastoma

Susanne Kleber,[1,10] Ignacio Sancho-Martinez,[1,10] Benedict Wiestler,[1,10] Alexandra Beisel,[1] Christian Gieffers,[6] Oliver Hill,[6] Meinolf Thiemann,[6] Wolf Mueller,[5] Jaromir Sykora,[8] Andreas Kuhn,[1] Nina Schreglmann,[1] Elisabeth Letellier,[1] Cecilia Zuliani,[1] Stefan Klussmann,[1] Marcin Teodorczyk,[1] Hermann-Josef Gröne,[2] Tom M. Ganten,[8] Holger Sültmann,[3] Jochen Tüttenberg,[9] Andreas von Deimling,[5] Anne Regnier-Vigouroux,[4] Christel Herold-Mende,[7] and Ana Martin-Villalba[1,*]
[1]Molecular Neurobiology Group
[2]Division of Cellular and Molecular Pathology
[3]Division of Molecular Genome Analysis
[4]INSERM U701
[5]KKE Neuropathology
German Cancer Research Center (DKFZ), INF 581, 69120 Heidelberg, Germany
[6]Apogenix GmbH, Heidelberg, 69120 Heidelberg, Germany
[7]Department of Neurosurgery
[8]Department of Internal Medicine
University of Heidelberg, INF 400, 69120 Heidelberg, Germany
[9]Department of Neurosurgery, University of Mannheim, Theodor-Kutzer-Ufer 1-3, 68167 Mannheim, Germany
[10]These authors contributed equally to this work.
*Correspondence: a.martin-villalba@dkfz.de
DOI 10.1016/j.ccr.2008.02.003

SUMMARY

Invasion of surrounding brain tissue by isolated tumor cells represents one of the main obstacles to a curative therapy of glioblastoma multiforme. Here we unravel a mechanism regulating glioma infiltration. Tumor interaction with the surrounding brain tissue induces CD95 Ligand expression. Binding of CD95 Ligand to CD95 on glioblastoma cells recruits the Src family member Yes and the p85 subunit of phosphatidylinositol 3-kinase to CD95, which signal invasion via the glycogen synthase kinase 3-β pathway and subsequent expression of matrix metalloproteinases. In a murine syngeneic model of intracranial GBM, neutralization of CD95 activity dramatically reduced the number of invading cells. Our results uncover CD95 as an activator of PI3K and, most importantly, as a crucial trigger of basal invasion of glioblastoma in vivo.

INTRODUCTION

The most frequent glioma (65%) is the glioblastoma multiforme (GBM), with a median survival of 10–12 months (Kleihues et al., 1993). Main obstacles to an effective therapy are invasion of migrating tumor cells into the normal surrounding brain tissue (host) and cellular resistance to multiple apoptotic stimuli. The CD95/CD95 Ligand (CD95L; Apo1L/FasL) death system is best described as an apoptosis inducer. Binding of trimerized CD95L to the CD95 receptor leads to recruitment of the adaptor protein FADD (Fas-associated death domain, MORT1) (Kischkel et al., 1995) and Caspase-8 and -10 into a death-inducing signaling complex (DISC) (Kischkel et al., 2001). FADD contains a death domain (DD) and a death-effector domain (DED). Via its DD, FADD binds to the DD of CD95 (Boldin et al., 1995). The DED recruits the DED-containing pro-Caspase-8 into the DISC, where it is activated through self-cleavage and commits the cell to apoptosis by activation of downstream effector caspases (Medema et al., 1997; Scaffidi et al., 1998). In this study we show that this signaling cascade is, however, absent in apoptosis-resistant GBM.

Src family kinases (SFKs) are nonreceptor tyrosine kinases participating in induction of GBM invasion (Park et al., 2006).

SIGNIFICANCE

Glioblastoma multiforme typically have diffuse, infiltrative growth patterns that hinder the achievement of complete surgical resection. Current treatment modalities aim at inducing apoptosis of remaining tumor cells in part by inducing expression of the death system CD95/CD95L. Overcoming resistance of tumor cells to CD95-induced apoptosis has been in the limelight of cancer research. We, however, found that tumor cells take advantage of CD95 to increase their infiltration capacity. Further, tumor cells even induce expression of the ligand for CD95 in the surrounding tissue. Thus, contrary to expectations, inhibition and not induction of the death system CD95/CD95L should be considered as frontline therapy for GBM.

SFKs activate phosphatidylinositol 3-kinase (PI3K) by direct phosphorylation of the regulatory subunit p85, as well as by phosphorylation of other proteins that can ultimately activate PI3K (Thomas and Brugge, 1997). Activation of SFKs involves interaction with partner proteins, as well as dephosphorylation of tyrosine residue 527 in the C-terminal domain (Tyr527). This provokes a conformational change allowing phosphorylation of tyrosine 416 in the activation loop (Tyr416), which is important for full activation of SFKs (Boggon and Eck, 2004).

We could show that in GBM samples from patients CD95L was highly expressed at the site of tumor/host interaction—the invasion front—by tumor cells and cells within the surrounding brain parenchyma, mostly neurons. A large population of GBM cells is, however, resistant to CD95-induced apoptosis. While current efforts are aimed at sensitizing these cells to CD95-mediated apoptosis, the possibility that CD95 might signal tumorigenesis has been largely ignored. Here, we detected an association of the Src family member Yes and the p85 subunit of PI3K to CD95. Activated PI3K leads to inhibition of glycogen synthase kinase 3-β (GSK3β) and induction of matrix metalloproteinases (MMPs). In intracranial GBM, neutralization of CD95 activity dramatically reduced the number of cells invading the contralateral hemisphere. Our study identifies CD95 as a major contributor to the invasion-prone phenotype of GBM and thus defines it as a prime target for future therapy.

RESULTS

CD95 Mediates Invasion of Glioblastoma Cells Resistant to Apoptosis

In established human malignant glioma cell lines, we first examined the induction of apoptosis upon triggering of CD95. The potency to activate CD95 proportionally correlates with the degree of oligomerization of CD95L. Since the available CD95L has a tendency to form aggregates, we engineered a human CD95L with a stable trimer-building capacity, the CD95L-T4 (Figure S1 available online). Different glioma cell lines exhibited different sensitivities to treatment with CD95L-T4: apoptosis was induced already at low concentrations in LN18 cells but not in T98G cells (Figure 1A). Specificity of CD95L-T4-induced death was tested by the neutralization of apoptosis by an antibody to CD95L (NOK1; Figure S3). Both LN18 and T98G cell lines, however, exhibited comparably high levels of CD95 surface expression (Figure 1A). These cell lines also expressed other molecules necessary for CD95-mediated apoptosis, such as FADD, Caspase-8, or Caspase-3 (Figures 5C and 5D) (Karmakar et al., 2006; Kugler et al., 2002).

Malignant glioma cells are characterized by their resistance to apoptosis, replicative potential, induction of angiogenesis, and migration/invasion. Stimulation of CD95 did not alter the proliferation rate of T98G cells (data not shown). We further examined CD95-induced migration through collagen-coated transwell inserts. Treatment with CD95L increased migration of T98G but not of LN18 cells (Figure 1B).

The migration of glioma cells requires cleavage of extracellular matrix components through MMPs. In T98G cells, MMP-9 activity, as assessed by gel zymography, increased upon treatment with CD95L-T4 (Figure 1C). Accordingly, stimulation of CD95 increased expression of MMP-2 and MMP-9 mRNA levels in the migration-prone T98G but not in the apoptosis-sensitive LN18 cells (Figures 1D and 1E). Most importantly, CD95-induced migration of T98G cells could be blocked with siRNA pool against MMP-2 and -9, indicating that these MMPs are required for CD95-induced migration (Figures 1F and 1G).

In a further series of experiments we used short-term glioma cultures derived from patients' tumors. These cells exhibited the typical GBM-genetic aberrations, including single-copy losses of the *PTEN* and *CDKN2a* loci and single-copy gain of the *c-erbB* (EGFR) locus, as assessed by array-CGH analyses (B. Radlwimmer, personal communication). Every primary GBM-derived culture examined here exhibited high CD95 surface expression (n = 18) and similar or higher levels of resistance to CD95-induced apoptosis (n = 8) compared to the ones observed in the invasion-prone T98G cell line (Figure 2A, Figure S2, and data not shown). Both the levels of CD95 surface expression and the resistance to CD95-mediated apoptosis were not affected by the number of passages in culture (data not shown). We further examined CD95-induced invasion in the GBM-derived cultures NCH89, NCH125, and NCH270. Triggering of CD95 in NCH125 and NCH270 increased expression of MMP-2 and MMP-9 and subsequently induced migration (Figures 2B–2D). Stimulation of CD95 in NCH89 cells increased neither migration nor expression of MMP-9 (Figures 2B–2D). Thus, the migration response to CD95 does not strictly correlate with the degree of resistance to apoptosis. Along the same line, expression of CD95 and CD95L mRNA differed among the highly invasive primary GBM tumors tested (Figure S2). MMPs are required for CD95L-T4-induced migration of NCH125, as a siRNA pool to MMP-2 and -9 significantly blocked migration (Figure 2E).

CD95 Mediates Invasion via the PI3K/GSK3β/MMP Pathway

One of the best described inducers of GBM invasion is EGF. Its binding to EGFR promotes MMP-9 expression through activation of the MAPK/ERK and the PI3K pathway (Rao, 2003). PI3K activates AKT/PKB, which in turn is able to phosphorylate GSK3β, leading to its inactivation. To test if PI3K or MAPK signaling could be responsible for the observed invasion, we determined phosphorylation of ERK and AKT. Stimulation of T98G and LN18 cells with CD95L-T4 activated AKT but not ERK (Figure 3A). Interestingly, ERK activity was even blocked with increasing time following stimulation (Figure 3A). In the invasion-prone T98G, NCH125, and NCH270 cells, phosphorylation of AKT exhibited a concentration-dependent bell-shaped curve (Figure 3B). In contrast, in NCH89 cells, which did not react to CD95 with increased invasion, CD95L-T4 did not activate AKT above basal levels (Figure 3B). Inhibition of GSK3β via phosphorylation at its serine-9 (phospho-ser9) was observed in T98G cells upon treatment with CD95L-T4 or αApo-1 antibody by western blot and FACS staining (Figure 3C and Figure S3).

Overexpression of a constitutively active GSK3β mutant (GSK S9A) via lentiviral infection blocked CD95-induced migration of T98G cells (Figure 3D). GSK S9A-expressing T98G cells and their wild-type counterparts exhibited comparable growth rate and levels of sensitivity to CD95-induced apoptosis (Figure S3). Thus, inhibition of migration by constitutively active GSK3β in T98G cells cannot be attributed to a different proliferation rate. Active GSK3β forms a complex with β-catenin, the adenomatous

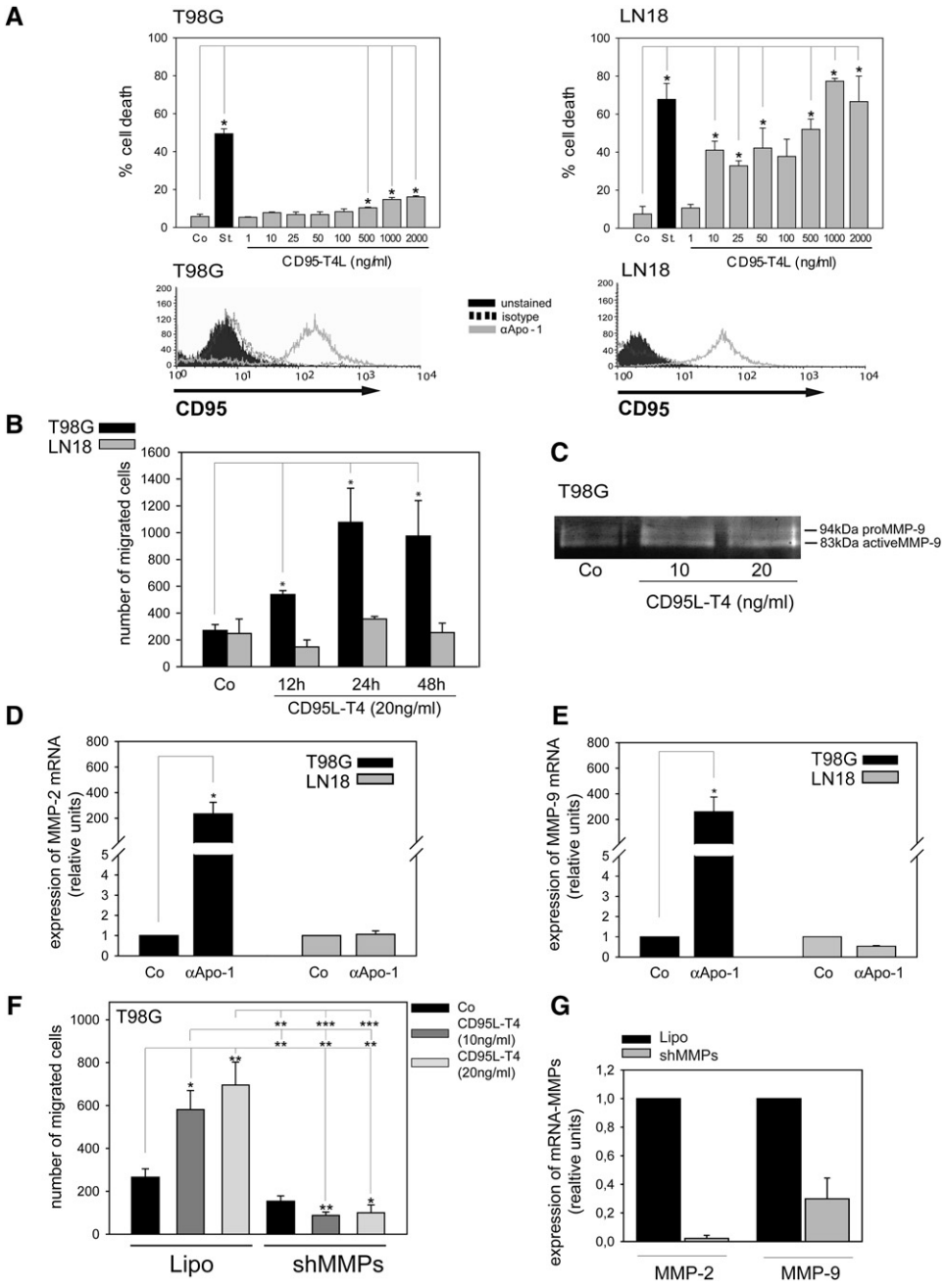

Figure 1. CD95 Triggers Invasion of Apoptosis-Resistant Cells via MMPs

(A) The glioblastoma cell lines T98G and LN18 were incubated with the indicated concentrations of CD95L-T4 or Staurosporin (St., 1 μM) or left untreated (Co). After 24 hr DNA fragmentation was analyzed by FACS (upper panel). (Lower panel) FACS analysis of CD95 surface expression in the T98G and LN18.

(B) T98G and LN18 cells were treated with CD95L-T4 or left untreated, to detect single-cell migration through a Boyden chamber with 8 μm pore size.

(C) T98G cells were treated with CD95L-T4 for 24 hr or left untreated. Thereafter, MMP-9 activity was assessed by Gel Zymography.

(D and E) T98G and LN18 cells were treated with αApo-1 for 48 hr or left untreated. Expression of MMP-2 and MMP-9 was measured by quantitative real-time PCR. Data are results from five independent experiments as mean ± SE, *$p < 0.05$.

(F) T98G cells were transfected with a siRNA pool against MMP-2 and MMP-9 (shMMPs) or with Lipofectamine alone (Lipo). Forty-eight hours after transfection, cells were treated with CD95L-T4; 48 hr afterwards migration was measured in a two-dimensional migration assay.

(G) Expression of MMP-2 and MMP-9 as measured by quantitative-RT-PCR.

(A, B, and D–F) Results are expressed as mean ± SE (*$p < 0.05$; **$p < 0.001$; ***$p < 0.0001$) and are representative of at least two independent experiments.

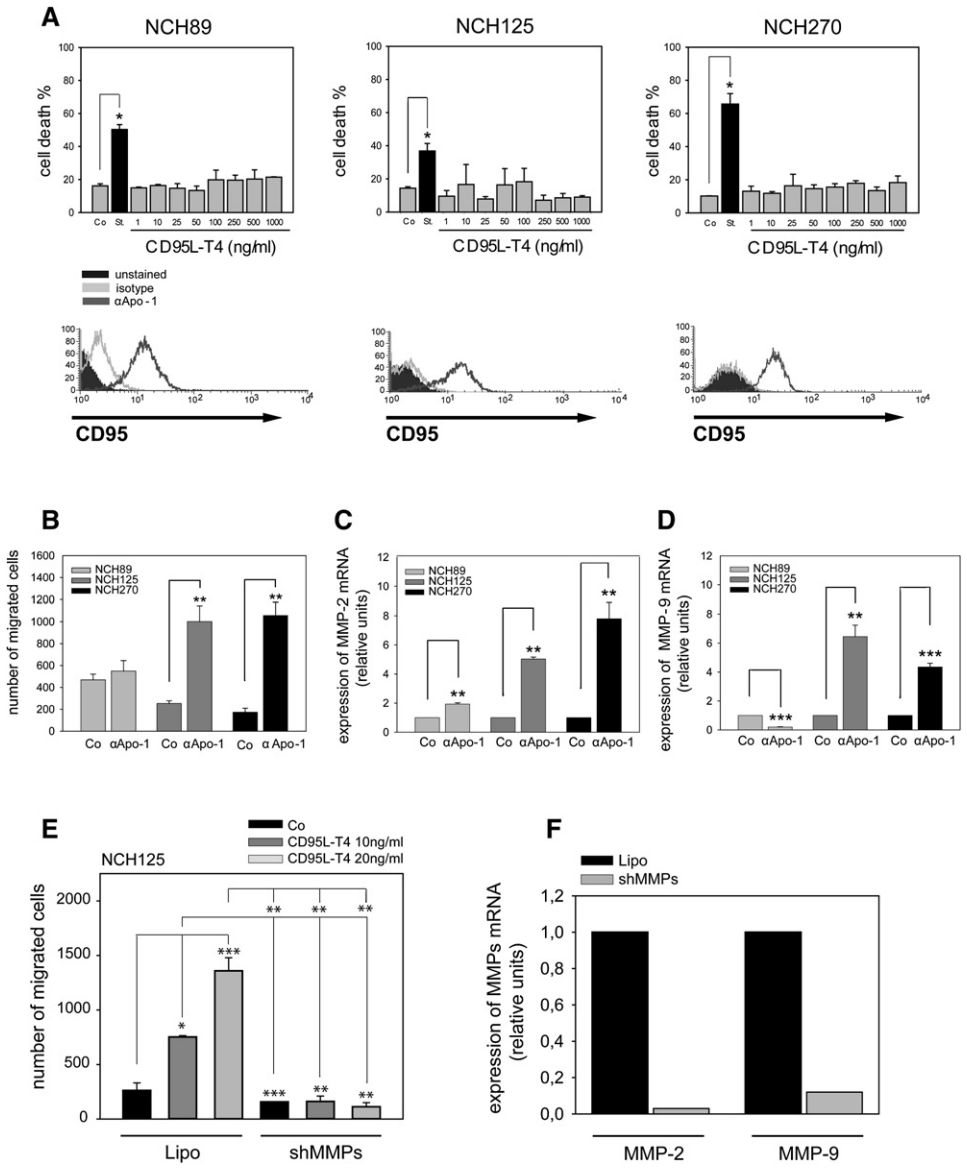

Figure 2. CD95 Triggers Invasion of Primary Apoptosis-Resistant Glioma Cells via MMPs

(A) The short-term cultured cell lines NCH89, -125, and -270 were incubated with the indicated concentrations of CD95L-T4 or Staurosporin (St., 1 μM) or left untreated (Co). After 24 hr DNA fragmentation was analyzed by FACS (upper panels). (Lower panels) FACS analysis of CD95 surface expression in the NCH89, -125, and -270.

(B) NCH cells were treated for 48 hr with αApo-1 or left untreated, to detect single-cell migration through a Boyden chamber with 8 μm pore size.

(C and D) NCH89, -125, and -270 cells were treated with αApo-1 for 48 hr. Expression of MMP-2 (C) and MMP-9 (D) was measured by quantitative real-time PCR.

(E) NCH125 cells were transfected with a siRNA pool against MMP-2 and MMP-9 (shMMPs) or with Lipofectamine alone (Lipo). Forty-eight hours after transfection, cells were treated with CD95L-T4, and migration was measured in a two-dimensional migration assay 48 hr later.

(F) Expression of MMP-2 and MMP-9 as measured by quantitative-RT-PCR. Results are expressed as mean ± SE (*$p < 0.05$; **$p < 0.001$; ***$p < 0.0001$) and are representative of at least two independent experiments.

polyposis coli (APC), and axin proteins—the degradation complex. Phosphorylation of β-catenin by GSK3β targets it for proteasomal degradation. As a consequence of GSK3β inhibition, β-catenin accumulates and translocates into the nucleus, where it engages the N terminus of DNA-binding proteins of the TCF (T cell factor)/Lef (lymphoid-enhancing factor) family (Eastman and Grosschedl, 1999), inducing expression of different target genes, including c-Jun, an essential transcription factor for MMP-9 expression (Gum et al., 1996; Sato and Seiki, 1993). Alternatively, inhibition of GSK3β activity can directly increase AP-1 expression (Troussard et al., 2000). To study whether stimulation of CD95 triggers β-catenin's transcriptional activity, we examined expression of cytoplasmic and nuclear β-catenin and β-catenin's transcriptional reporter activity. LiCl, a known inhibitor of GSK3β and inducer of β-catenin's transcriptional activity, was used as a positive control. In T98G cells, triggering

of CD95 induced cytoplasmic accumulation of β-catenin 30 min after stimulation with CD95L-T4 (Figure 3E). Further, nuclear translocation of active β-catenin, nonphosphorylated on the GSK-targeted Ser 37 or Thr 41, was observed (Figure 3F). TCF/Lef-reporter activity (TOP-FLASH) was also significantly induced upon CD95L-T4 (Figure 3G). Mutation of the TCF/Lef-binding domain abolished CD95L-T4 induction of luciferase activity (FOP-FLASH; Figure 3G). Additionally, activity of NFκB increased significantly 8 hr after stimulation with 20 but not 10 ng/ml CD95L-T4 (Figure 3H). Taken together, activation of CD95 induces migration/invasion through the PI3K/AKT/GSK3β/β-catenin/MMP and possibly the PI3K/AKT/NFκB/MMP pathway. Involvement of the latter pathway will be the subject of future studies.

PI3K Is Activated via Recruitment of Src to CD95

As CD95 is not a receptor tyrosine kinase, a promising candidate connecting CD95 to PI3K could be a nonreceptor tyrosine kinase of the Src family kinases. To investigate whether Src connects CD95 to PI3K activity, we performed coimmunoprecipitation experiments (Figures 4A–4C). Indeed, treatment of T98G and LN18 cells with CD95L-T4 induced recruitment of Src and the p85 subunit of PI3K to CD95. Association of p85 with CD95 was examined by immunoprecipitating either CD95 or p85. The degree of association of p85 with CD95 inversely correlated with the concentration of CD95L-T4 in T98G cells (Figure 4B). However, in LN18 cells p85 recruitment to CD95 was only detected at high concentrations of CD95L-T4 (Figure 4A). Immunoprecipitation of CD95 allowed detection of a Src family member at 5 min after treatment with low concentration of CD95L-T4 (Figures 4A and 4B). Src association decreased at a higher concentration (Figures 4A and 4B). Thus, at low concentrations of CD95L-T4 both Src and p85 associated at detectable levels with CD95 in T98G cells, but in LN18 cells only Src was detected. Further, after a screening with antibodies to several SFKs, such as Fyn, Lyn, pp60, and Yes, we identified Yes as the Src family member that links CD95 to PI3K (Figure 4C). To validate the role of Yes in the migration of glioma cells, knockdown experiments were performed. In cells transfected with Yes siRNA, expression of Yes, as assessed by FACS and qRT-PCR, was reduced, while Fyn expression, another Src family member, remained unaffected (Figure 4E). siRNA to Yes, but not to Fyn, significantly abolished CD95L-T4-induced migration of T98G and of NCH125 cells (Figure 4D). This block of migration was rescued by Yes overexpression in T98G and LN18 cells (Figure 4F). Like the PI3K inhibitor LY290059, siRNA to Yes also inhibited CD95-induced phosphorylation of AKT (Figure 4G).

Inefficient DISC Formation in Apoptosis-Resistant Glioma Cells

If Yes and p85 get recruited to CD95 in both apoptosis-prone and -resistant cells, what determines the fate of the cell? To address this issue, we examined the role of the PI3K pathway repressor PTEN (MMAC1, TEP1). While the apoptosis-prone LN18 cells have an intact PTEN, T98G cells carry a point mutation (codon 42 CTT to CGT; Glycine to Glutamine) in one allele and lack of the second allele of *PTEN* and a total loss of one of the chromosomes 10 (Fan et al., 2002; Furnari et al., 1997). PTEN overexpression, however, did not sensitize T98G or NCH125 cells to CD95-mediated apoptosis (Figure 5A).

We further questioned whether caspases were involved in CD95-induced activation of PI3K. Inhibition of caspases by the general caspase inhibitor zVAD-fmk did not prevent GSK3β phosphorylation (Figure 5B). Likewise, CD95-induced cleavage of Caspase-8 could only be detected in LN18 but not in T98G cells (Figure 5C). To investigate if DISC components were efficiently recruited in these cells, we analyzed FADD recruitment in CD95-immunoprecipitates. Whereas upon stimulation with CD95L-T4 recruitment of FADD to CD95 increased in LN18 cells, no increase was detected in T98G cells (Figure 5D). Accordingly, Caspase-8 recruitment to CD95 increased upon stimulation with CD95L-T4 in LN18 and J16 cells but not in T98G cells (Figure 5D). Most importantly, in T98G cells, siRNA knockdown of Yes enabled CD95L-T4 induction of FADD recruitment to CD95 (Figure 5E). Along this line, while expression levels of FADD were similar in LN18 and T98G cells, Yes levels were significantly higher in T98G cells (Figure 5F). As opposed to Yes, Fyn expression was significantly higher in LN18 cells (Figure 5F). Taken together, we propose that CD95 mediates invasion via the Yes/PI3K/AKT/GSK3β/MMP pathway (Figure 6).

The CD95/CD95L System Is an Important Mediator of Glioma Invasion In Vivo

Expression of CD95L in patients suffering from GBM showed a triangle-like distribution of CD95L in every tumor examined (Figure 7A). Inside the tumor, only small amounts of CD95L were expressed (Figure 7Aa). Expression increased at the tumor/host interface, peaked in the brain parenchyma adjacent to the tumor (Figure 7Ab), and decreased again with increasing distance to the glioma (Figure 7Ac). CD95L was detected in tumor cells, neurons, and macrophages (data not shown). Additional expression of CD95L within the tumor was observed in glioma cells surrounding tumor vessels. Likewise, phosphorylation of Src family kinases (pSrc) and Yes expression were consistently found at the tumor/host interface in every examined sample, suggesting a role in tumor invasion (Figure 7B). Within solid tumor areas, expression of Yes highly varied between tumor samples, from very high to expression only in scattered tumor cells. In these highly Yes-expressing areas phosphorylation of Src was either not detected or rather limited (Figure 7B).

For translation of our findings into a more physiological in vivo setting, we examined the role of the CD95/CD95L system in a mouse model of GBM. For these studies, the established murine glioma cell line SMA-560 was injected intracranially into a syngeneic Vm/Dk host (Ashley et al., 1998). The use of a syngeneic tumor model was important to allow the tumor's induction of CD95L expression in the surrounding brain tissue.

SMA-560 cells expressed only low levels of CD95 receptor on their surface (Figure 8A) and no CD95L at all (Figure 8B), when kept under cell culture conditions. As reported by others (Ashley et al., 1998), we found SMA-560 cells to be resistant to CD95-induced apoptosis (data not shown). Following formation of spheroids, the levels of CD95 slightly increased (Figure 8A), whereas FACS analysis failed to identify CD95L at the cell surface (Figure 8B). Despite the relatively low CD95 surface levels, spheroids of these cells displayed increased migration in the collagen invasion assay after CD95 stimulation in a concentration-dependent manner

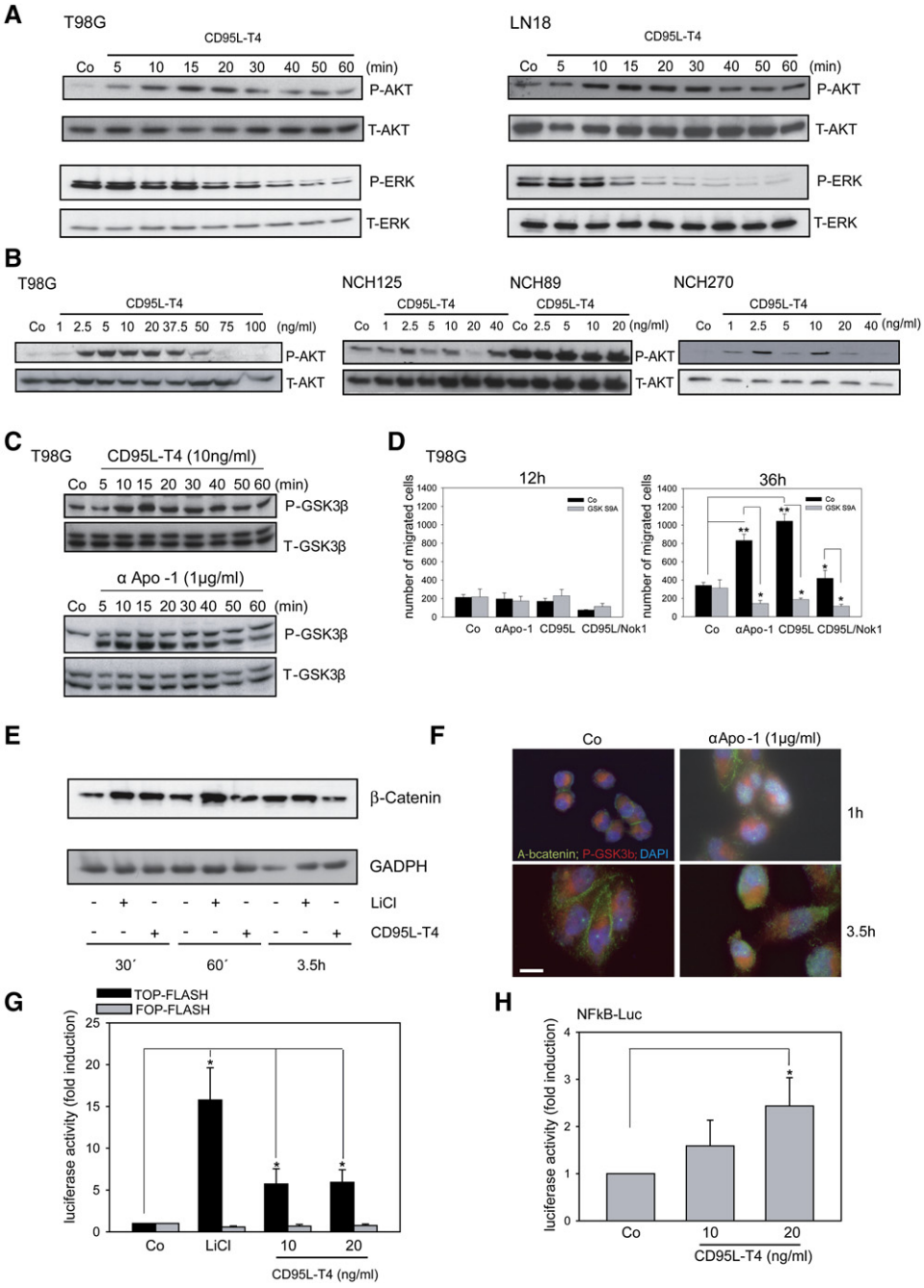

Figure 3. CD95 Induces Migration via the PI3K/AKT/GSK3β Pathway

(A) Phosphorylation of AKT and ERK is shown in T98G and LN18 cells upon treatment with CD95L-T4 at the indicated time points.

(B) In T98G, LN18, and NCH125 and -270 cells, but not in NCH89, phosphorylation of AKT exhibited a concentration-dependent bell shape after stimulation with CD95L-T4.

(C) In T98G cells, treatment with CD95L-T4 (10 ng/ml) and αApo-1 (1 μg/ml) induced GSK3β phosphorylation. Kinetics of GSK3β inhibition exhibited a bell-shaped curve.

(D) T98G cells were infected with an empty lentiviral vector (Co) or a constitutively active GSK3β mutant (GSK S9A). At 36 hr GSK S9A-infected T98G cells migrated significantly less than their empty vector counterparts upon treatment with αApo-1 or CD95L. A neutralizing antibody to CD95L (Nok1) blocked CD95L-induced migration of vector- and GSK S9A-infected cells. Results are expressed as mean ± SE (*$p < 0.05$; **$p < 0.001$) and are representative of two independent experiments.

(E) β-Catenin accumulated in the cytosol of T98G cells 30 min after treatment with CD95L-T4 (10 ng/ml).

(F) Active β-catenin (green) translocated into the nucleus upon stimulation with αApo-1. DAPI (blue) and P-GSK3β (red) were used to visualize the nuclei and the cytosol, respectively, in T98G cells.

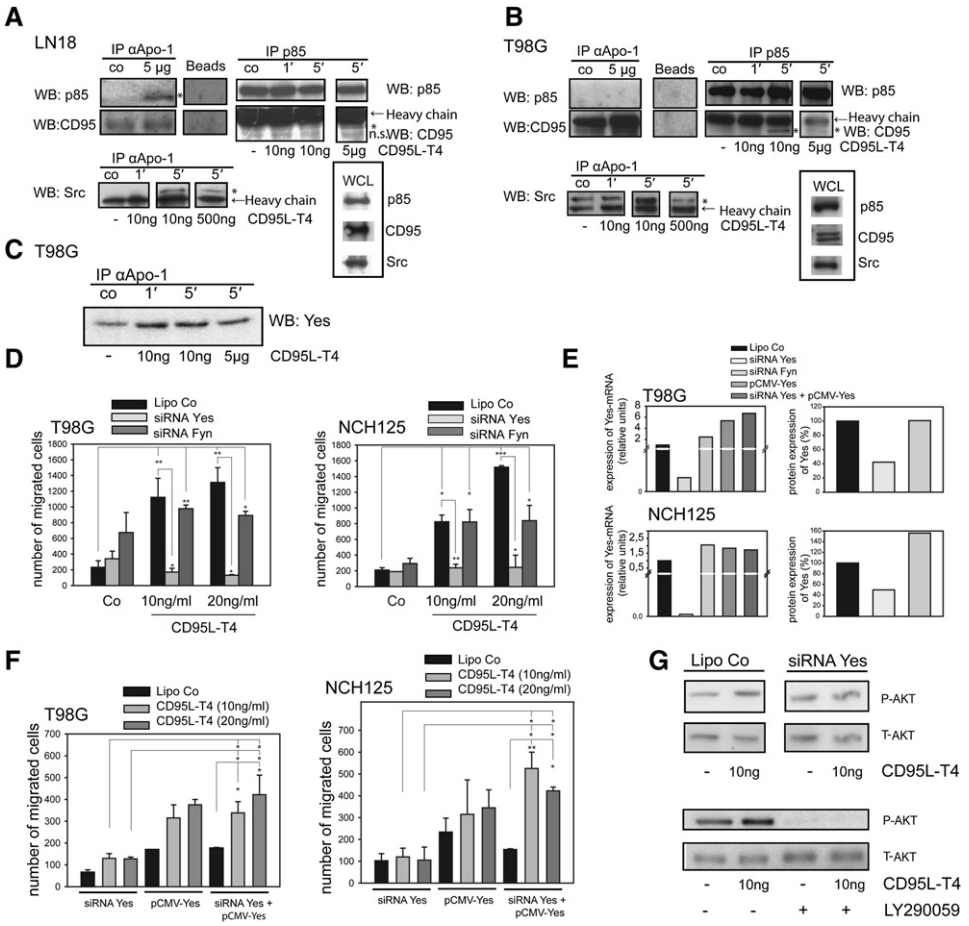

Figure 4. Src and p85 Associate to CD95 to Activate AKT

(A and B) LN18 and T98G cells were stimulated with CD95L-T4 for the indicated time points and concentrations. (Left panels) CD95 was immunoprecipitated, and the immunoprecipitates were immunoblotted with anti-p85, anti-CD95, and anti-Src antibodies. (Middle panels) p85 was immunoprecipitated, and the immunoprecipitates were probed with anti-p85 and anti-CD95 antibodies. Protein-A beads are included as a negative control. Whole cellular lysates (WCL) probed with anti-p85, anti-CD95, and anti-Src are shown on the right panels.

(C) T98G cells were treated for the indicated times and concentrations with CD95L-T4. CD95 was immunoprecipitated, and immunoprecipitates were immunoblotted with anti-Yes antibody.

(D) T98G and NCH125 cells were transfected with siRNA against Yes or Fyn or with Lipofectamine alone (Lipo). Seventy-two hours after transfection, cells were treated with CD95L-T4, and 24 hr afterwards migration was measured in a two-dimensional migration assay.

(E) Expression of Yes-mRNA as measured by quantitative-RT-PCR and Yes protein levels as assessed by FACS analysis are shown.

(F) T98G and NCH125 cells were transfected with siRNA against Yes, a Yes overexpression plasmid (pCMV-Yes), or both. Seventy-two hours after transfection, cells were treated with CD95L-T4, and 24 hr afterwards migration was measured in a two-dimensional migration assay.

(G) Yes siRNA and the PI3K inhibitor (LY 290059) blocked CD95-induced phosphorylation of AKT. P, phosphorylated; T, total; *specific band; n.s., unspecific band.

(D and F) Results are expressed as mean ± SE (*$p < 0.05$; **$p < 0.001$; ***$p < 0.0001$) and are representative of two independent experiments.

(Figure 8C). In accordance with our finding that spheroids do not express CD95L (Figure 8B), blockage of CD95L using the CD95L-neutralizing antibody MFL3 did not alter invasion (Figure 8C).

Interestingly, when cells isolated from solid tumors were analyzed 14 and 18 days after inoculation, surface levels of CD95 and CD95L significantly increased (Figures 8A and 8B). This indicates the requirement of tumor/host interaction and, therefore, of a crosstalk between host factors and tumor cells as given in the case of murine GBM-model.

For a more detailed analysis of the functional significance of this increase, we extracted fragments from solid tumors 14 days after intracranial injection of cells. These cells were preincubated with either medium alone, medium with CD95L-neutralizing antibody (MFL3), or the appropriate isotype antibody, respectively. After embedding into collagen gels, migration was monitored for a period of 72 hr (Figure 8D). Strikingly, preincubation with the CD95L-neutralizing antibody MFL3, but not with the isotype or medium alone, reduced migration

(G and H) Twenty-four hours after transient transfection of T98G with the β-Catenin/TCF transcriptional reporter (TOP-FLASH; [G]), the control plasmid (FOP-FLASH; [G]), or the NFκB-reporter construct (NFκB-Luc; [H]); cells were treated with CD95L-T4 (G and H) or LiCl (G), or left untreated (G and H). Luciferase activity was assayed 12 hr (G) or 8 hr (H) afterwards and normalized to renilla luciferase expression. P, phosphorylated; T, total. Scale bar, 20 µm.

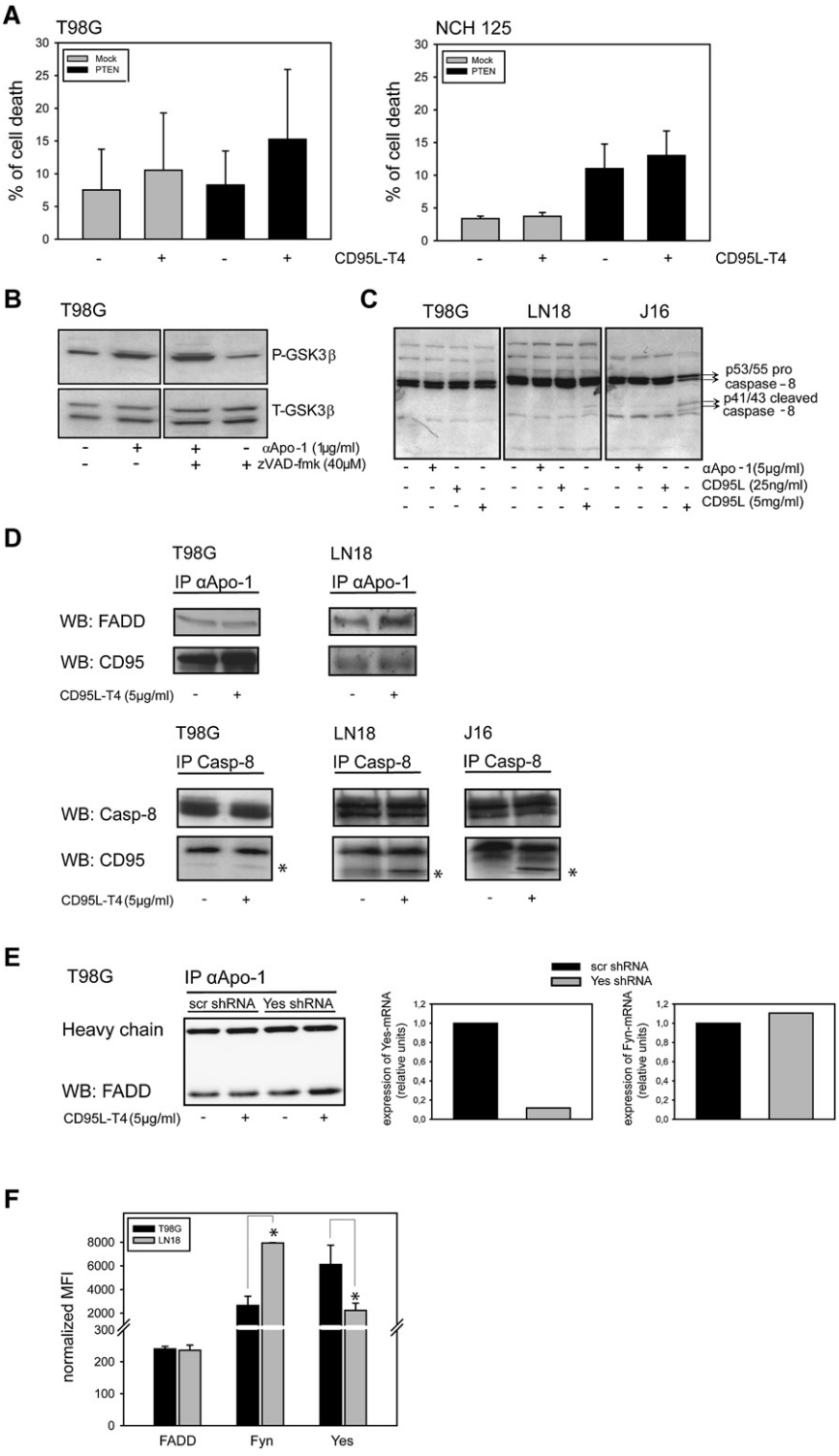

Figure 5. Inefficient DISC Formation in Apoptosis-Resistant Glioma Cells

(A) Forty-eight hours after transient transfection of T98G and NCH125 with either a HA-PTEN (PTEN) or the empty vector (Mock), cells were treated with CD95L-T4 (500 ng/ml). To detect cell death in PTEN-overexpressing cells, an intracellular FACS staining against the HA-tag was performed. Thereafter, forward side scatter analysis was performed in HA-positive cells. Results are expressed as mean ± SE and are representative of two independent experiments.

(B) T98G cells were treated for 1 hr with αApo-1, zVAD-fmk, or a combination of zVAD-fmk and αApo-1, or left untreated (Co). Phosphorylation of GSK3β was analyzed by western blot.

(C) Cleavage of Caspase-8 in T98G, LN18, and Jurkat 16 (J16) was detected by western blot analysis at 5 min after CD95 stimulation.

(D) In T98G and LN18 cells treated with CD95L-T4 for 5 min, either CD95 (upper panels) or Caspase-8 (lower panels) was immunoprecipitated. The immunoprecipitates were immunoblotted with anti-FADD antibody and anti-CD95 (upper panels) and with anti-CD95 and anti-Caspase-8 (lower panels). Jurkat cells were included as a positive control.

(E) T98G cells were transfected with either Yes shRNA or a nontargeting shRNA as a negative control. After 72 hr, cells were treated with CD95L-T4 or left untreated, and immunoprecipitation of CD95 was performed; the immunoprecipitates were then immunoblotted with anti-FADD antibody, and the IgG heavy chain serves as loading control. On the right, knockdown efficiency assessed by quantitative-RT-PCR is shown.

(F) Quantitative expression of FADD, Yes, and Fyn in T98G and LN18 cells was measured by FACS analysis. Results are expressed as mean ± SD (*$p < 0.05$) and are representative of three independent experiments. MFI, mean fluorescence intensity; P, phosphorylated; T, total.

of cells out of the tumor core by approximately 50% (Figure 8D).

To verify these results in vivo, we injected GFP-positive SMA-560 cells and MFL3 or the appropriate isotype antibody into the left striatum of Vm/Dk mice. Treatment with MFL3 significantly reduced migration of tumor cells into the contralateral hemisphere (Figure 8E). We conclude from these data that the CD95/CD95L system is a major mediator of malignant glioma invasion into the surrounding brain in vivo.

DISCUSSION

The CD95/CD95L system is generally appreciated for its role in inducing apoptosis (Krammer, 2000). However, evidence accumulates that CD95 can mediate apoptosis-independent processes such as proliferation, angiogenesis, fibrosis, and inflammation (Biancone et al., 1997; Hohlbaum et al., 2002). Overexpression of CD95 in Lewis lung carcinoma cells resulted in a survival advantage of tumor cells in vivo (Lee et al., 2003). Along the same line, triggering of CD95 has been reported to drive cell-cycle progression in glioma cells (Shinohara et al., 2000). In malignant astrocytoma, CD95 ligation promoted

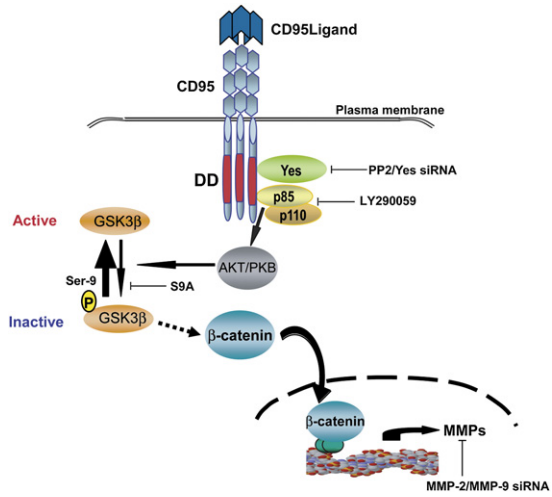

Figure 6. Schematic Model for CD95 Signaling of Invasion in Glioblastoma

CD95L induces recruitment of the Src family member Yes and the p85 subunit of PI3K (depicted here by its two subunits: p85 and p110) to CD95, thereby activating AKT. Activated AKT phosphorylates and inactivates GSK3β, allowing β-catenin translocation into the nucleus, where it induces transcription of MMPs. This signaling pathway could be blocked by siRNA against Yes, or MMP-2 and -9, the PI3K-specific inhibitor (Ly290059), or by lentiviral infection with a dominant-active mutant of GSK3β (S9A).

expression of proinflammatory chemokines and angiogenesis (Choi et al., 2001, 2002, 2003). Here, we report that triggering of CD95 in glioblastomas initiates a cascade of signaling events ultimately leading to increased migration. CD95-induced migration was first observed in cultured renal tubular cells (Jarad et al., 2002) and has recently been reported for ovary, breast, lung, and kidney tumor cells (Barnhart et al., 2004). In the latter study, a serum gradient was added to the CD95 stimulus in order to instigate and direct cell migration (Barnhart et al., 2004). Glioblastoma cells, on the contrary, are characterized by their invasion-prone phenotype and do migrate in the absence of an additional stimulus. This highly invasive behavior could be blocked in vitro, ex vivo, and in vivo by the sole neutralization of CD95 activity, indicating that CD95/CD95L contributes to the invasion-prone phenotype of malignant glioma cells.

To invade and spread into the surrounding normal brain, tumor cells need to digest components of the extracellular matrix (ECM), including fibronectin, laminin, and type IV collagen. The best characterized family of ECM-degrading enzymes is the MMP family. MMP-9-deficient glioblastomas are less invasive in vitro and in vivo (Rao, 2003). Glioblastomas produce significantly higher levels of MMP-9 than do lower-grade gliomas and normal brain tissue (Rao, 2003). Levels of MMP-9 increased during the growth of glioblastoma cells that had been implanted intracranially in nude mice (Sawaya et al., 1998). Furthermore, these proteases play a role in establishing and maintaining a microenvironment that facilitates tumor cell survival. Accordingly, MMPs regulate tumor angiogenesis, and inhibition of MMP-9 reduced capillary-like structures in mixed cultures of endothelial and glioma cells (Rao, 2003). The same features hold true for CD95L expression: (1) levels positively correlate with the degree of malignancy (Choi et al., 2001; Frei et al., 1998; Weller et al., 1994); (2) levels increase after intracranial inoculation; (3) in human specimens of GBM, one of its preferential localizations is at the tumor vessels. Here we show that triggering of CD95 greatly increases mRNA expression of MMP-9 and MMP-2 in established glioblastoma cell lines and primary cultures, and knockdown of MMP-2 and MMP-9 blocks CD95-induced migration. The promoter region of MMP-9 contains putative binding sites for AP-1, NFκB, Sp1, and AP-2 (Sato and Seiki, 1993). The AP-1 transcription complex plays an essential role in stimulating transcription of MMP-9 (Gum et al., 1996; Sato and Seiki, 1993). c-Jun, a putative component of the AP-1 transcription complex, has been identified as one of the most highly induced TCF/β-catenin target genes (Mann et al., 1999; Staal et al., 2004). Inhibition of GSK3β, as reported here, allows unphosphorylated β-catenin to accumulate and translocate into the nucleus, where it functions as a cofactor for transcription factors of the TCF/Lef family (Reya and Clevers, 2005). In addition, activity of NFκB was concomitantly observed. Since CD95L-T4 decreases ERK activity, we believe that in T98G cells AKT regulates NFκB activity through phosphorylation/activation of the IKK kinase, which in turn phosphorylates IκB and allows the release of activated NFκB (Ozes et al., 1999). Alternatively, IκB can transactivate the p65 subunit (Madrid et al., 2000). In contrast, the induction of motility and invasiveness previously reported for tumor cell lines of endodermal or mesodermal origin involves ERK and Caspase-8 activity (Barnhart et al., 2004). Thus, activation of CD95 induces migration/invasion through the PI3K/AKT/GSK3β/β-catenin/MMP and perhaps the PI3K/AKT/NFκB/MMP pathway.

In the past, several reports have pointed out an important role for tyrosine phosphorylation in CD95-induced signaling (Eischen et al., 1994; Schlottmann et al., 1996). These preliminary reports, however, suggested that CD95-induced tyrosine phosphorylation is a prerequisite for CD95-mediated apoptosis (Eischen et al., 1994; Gulbins et al., 1998; Schlottmann et al., 1996). Along this line, the phosphatases SHP-1, SHP-2, and SHIP were found to associate with CD95 to counteract survival factor-initiated pathways (Daigle et al., 2002). Just recently, Src-induced tyrosine phosphorylation of Caspase-8 was found to impair CD95-induced apoptosis (Cursi et al., 2006). We now describe association of the Src family member Yes and p85 with CD95. TRANCE, another TNF family member, activates PI3K through a signaling complex involving c-Src and TRAF6 (Wong et al., 1999). Inhibition of Fyn, another Src family member, decreased CD95-induced migration of glioblastoma cells, although not significantly. This can be explained by the fact that Fyn is involved in EGFR-mediated signaling in neural cells (Stirnweiss et al., 2006) and EGFR is a very important receptor for glioma invasion that has been found in association with CD95 (Eberle et al., 2005). Thus, inhibition of CD95-mediated signaling might affect EGFR-mediated signaling and vice versa. Whether another adaptor molecule is still missing in CD95's PI3K-activation complex (PAC) remains a subject for future studies. Alternatively, Yes and p85 might directly interact with CD95. Accordingly, in T98G cells, knockdown of Yes enabled CD95L-T4-induced recruitment of FADD to CD95, indicating that Yes and FADD might compete for binding to CD95. Along this line, analysis of Yes expression levels revealed a much higher expression in T98G than in LN18 cells. Most importantly, expression of Yes and phosphorylation of Src family kinases was consistently found

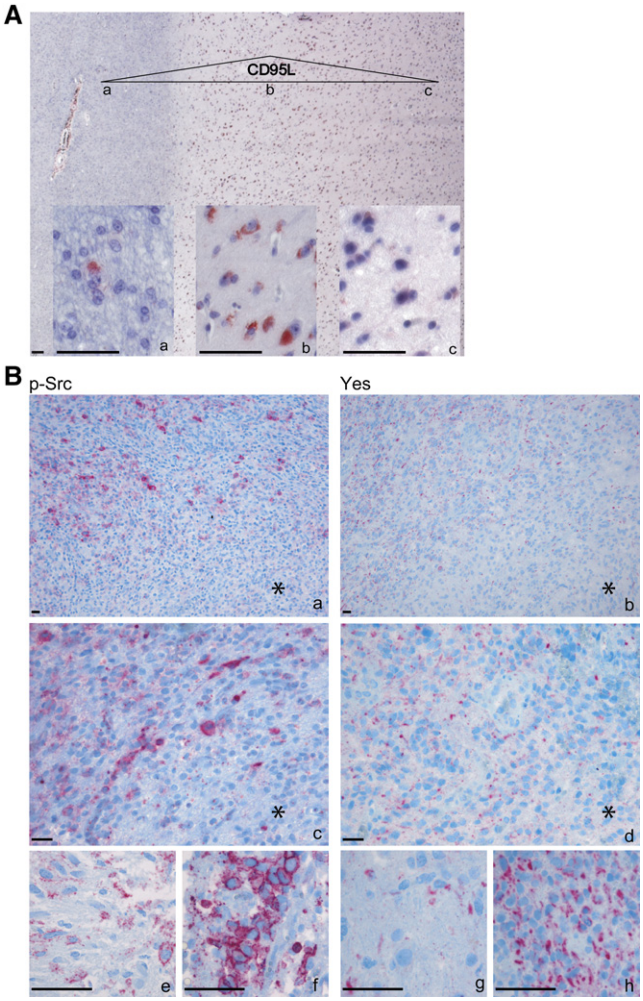

Figure 7. Expression of CD95L, Yes, and Phospho-Src in Clinical Samples of GBM

(A) Representative immunohistochemical staining of CD95L (red) in primary human GBM. Note the increased expression of CD95L at the tumor/host interface (Ab) compared to more solid tumor areas (asterisk in [Aa]) or brain parenchyma (Ac).

(B) Immunohistochemical staining of phosphorylated Src family kinases (p-Src; [Ba, Bc, Be, and Bf]) and Yes (Bb, Bd, Bg, and Bh). (Ba–Bd) Overview of tumor infiltration zone; note robust phosphorylation of Src and expression of Yes in zone of tumor/host interaction (to the left) and reduced or no p-Src in solid tumor areas (to the right, as indicated by the asterisk). Yes expression was found at the tumor/host interface (Bb, Bd, and Bg) and in scattered solid tumor areas (Bh). Strong phosphorylation of Src in tumor cells in solid tumor areas (Bf) and infiltration zone (Be). Scale bar, 50 μm.

at the site of tumor/host interaction in clinical samples of GBM, indicating its involvement in tumor invasion.

Barnhart et al. (2004) previously showed that exogenous CD95L induces migration of tumor cells from endodermal origin in vitro. In these cells CD95L induces migration via Caspase-8 and ERK (Barnhart et al., 2004). These authors speculate that CD95L might be involved in the tumor's escape from chemo- and radiotherapy, since both treatments increase expression of CD95L. In our study we found that CD95L also induces migration of GBM cells. Beyond this, the present study represents a significant conceptual advance in the field of tumor biology because it shows that: (1) the sole interaction of tumor cells with the surrounding parenchyma induces expression of CD95L in tumor and host cells; (2) in GBM cells CD95L signals invasion via Yes/PI3K/MMPs and not via Caspase-8/ERK, as it is the case in tumor cells of endodermal origin; (3) neutralization of CD95 activity blocks the basal migration of GBM cells in vivo in a mouse syngeneic model of GBM that mimics the clinical situation. In addition, this study shows that the molecular stoichiometry of the PI3K signaling components seems to determine the cellular response to CD95.

In summary, our data indicate that, generally, WHO IV tumors are resistant to CD95-induced apoptosis and instead increase their invasion capacity upon stimulation of CD95. Current experimental strategies targeting glioblastoma invasion focus on inhibition of MMP activity by expression of the natural inhibitors TIMP2 and TIMP4 or are based on direct gene targeting of MMP mRNA by antisense strategies. Nevertheless, while TIMP2 decreases angiogenesis and invasion, it also protects tumor cells from apoptosis (Valente et al., 1998). Other strategies to inhibit MMP production employ targeting the signal transduction pathways leading to their expression, which, however, are involved not only in the induction of tumor invasion, but also in some basic physiologic functions, thus making these strategies less attractive for clinical application. While CD95 activity is required for neurite remodeling during embryonic brain development (Zuliani et al., 2006) and for the clearance of damaged cells in the diseased brain (Demjen et al., 2004; Martin-Villalba et al., 1999, 2001; Mattson, 2000), no CD95 protein is detectable in the healthy adult brain. Thus, targeting CD95 should have fewer side effects than other migration-inducing factors that are normally involved in normal brain function.

Here, we provide evidence that CD95 directly activates PI3K to contribute to the invasion-prone phenotype of GBM. Considering that current treatments of GBM are not successful because of the highly invasive nature of these brain tumors, finding another therapeutic approach is of prime importance.

Here, we provide evidence that targeting the CD95/CD95L system holds promise for the frontline therapy of human GBM.

EXPERIMENTAL PROCEDURES

Primary Samples

Tissue specimens of NCH tumors were obtained intraoperatively. Informed consent was obtained from each patient according to the research proposals approved by the Institutional Review Board at the Medical Faculty Heidelberg. Fresh tissue was divided into two parts, one part to establish primary tumor cultures and the other for RNA extraction.

Knockdown Experiments

Knockdown experiments were performed by transient transfection of siRNA pools (Dharmacon) with Lipofectamine 2000 (Invitrogen Life Technologies) following the instruction manual. Migration experiments were performed using either validated siRNA against Yes (QIAGEN SI00302218), and a second siRNA, targeting a different member of the Src family kinases, Fyn (QIAGEN SI00605451), which was used as a negative control, or pools of validated shRNAmir-pGIPZ-vectors for Yes, MMP-2, and MMP-9 and a nontargeting shRNAmir-pGIZ vector as a negative control (RHS 4430-98843955, -98820654, -99161516, -98514235, -98709361, -99137419, -99291751, -99298712, and -99138418, and RHS 4346-OB, respectively; Open

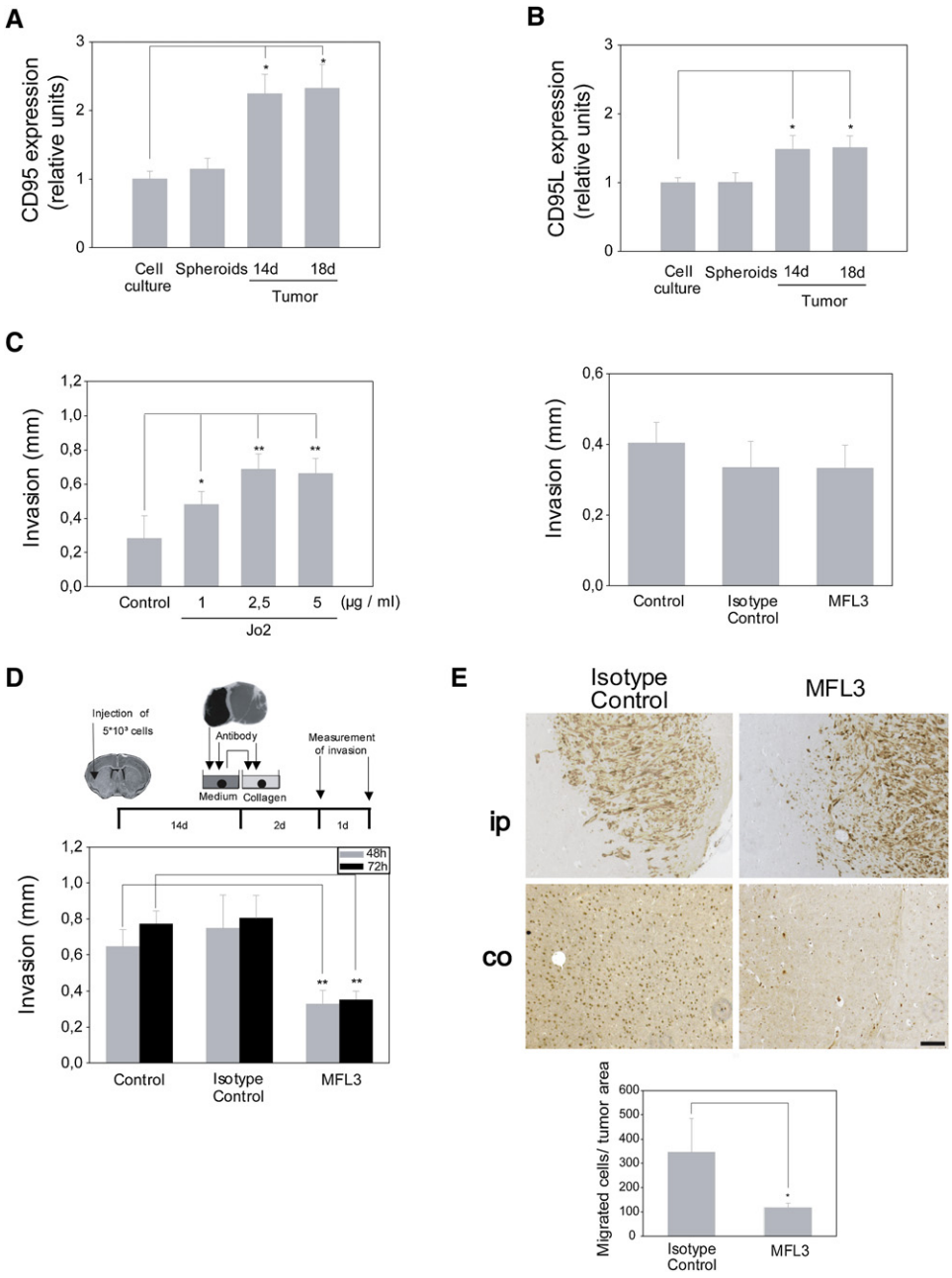

Figure 8. CD95 and CD95L Are Upregulated on Murine Glioma Cells In Vivo and Induce Migration

(A and B) CD95 and CD95L surface expression on the murine glioma cell line SMA-560 was determined under normal cell culture conditions, after the formation of spheroids or following intracranial implantation. Changes were normalized to cell culture condition levels. Results represent three independent experiments and are expressed as mean ± SD (*$p < 0.05$).

(C) Spheroid cultures were embedded into a collagen matrix and treated with antibodies to CD95 (Jo2), a neutralizing antibody to CD95L (MFL3), or the appropriate isotype control antibody at the indicated concentrations. The migration of cells was monitored over 48 hr, and the distance of cells to the spheroid's border is depicted (n = 10 cells, three spheroids per treatment).

(D) Experimental scheme. Migration of tumor explants into collagen after treatment with either MFL3 or the appropriate isotype control is depicted as described above (n = 10, three spheroids per treatment).

(E) Representative pictures of GFP-immunostained isotype- or MFL3-treated SMA tumors. The tumor-bearing (ipsilateral) and contralateral hemispheres are shown. Numbers of SMA-560 cells (GFP-positive) in the contralateral hemisphere of Vm/Dk mice treated with either MFL3 or the isotype control antibody were counted and normalized to tumor area. Shown results are representative of two independent experiments and expressed as mean ± SD (*$p < 0.05$; **$p < 0.001$). Scale bar, 100 µm.

Biosystems, USA). After transient transfection with the different siRNAs, cells were cultured for 72 hr before treatment with CD95LT4 (10 ng/ml and 20 ng/ml), and migration was analyzed 24 hr after treatment with a two-dimensional migration assay. The knockdown was controlled by quantitative real-time PCR and FACS. To exclude off-target effects of Yes-siRNA, cells were transfected with siRNA against Yes, a Yes overexpression plasmid (p-CMV-Yes), or both and cultured for 48 hr before being transferred to a migration plate. After an additional 48 hr, cells were treated with CD95L-T4 (10 ng/ml and 20 ng/ml). Migration was measured 24 hr after treatment in a two-dimensional migration assay.

For immunoprecipitation studies, transfected cells were cultured for 72 hr prior to treatment.

Animal Experiments

All animal experiments conform to the relevant regulatory standards and have been approved by the ethical authorities (Regierungspräsidium Karlsruhe, Germany). For intracranial injections, 8- to 12-week-old inbred Vm/Dk mice were used. 5.000 SMA-560 cells were harvested by trypsinization, resuspended in 1 μl DMEM supplemented with 10% FCS, 1% penicillin/streptomycin (PS), and 1% L-Glutamine (200 mM) and loaded into a 10 μl Flexilfil syringe (WPI, Berlin, Germany). A burr hole was drilled 2.75 mm lateral to the bregma, and the needle was introduced to a depth of 3 mm. Mice were sacrificed 7, 14, or 18 days after injections.

Tumor Explants

Fourteen days after tumor inoculation, the mice were sacrificed, and the tumors were extracted. Tumor explants were then incubated for 1 hr in either medium, medium plus isotype control antibody (IgG 10 μg/ml), or medium with MFL3 (10 μg/ml). Following embedding of the explants into collagen, cell invasion was recorded over 72 hr with a time-lapse microscope (Olympus, Germany).

Tumor Analysis

For analysis of CD95-induced migration in vivo, a suspension of 5.000 SMA-560-GFP cells and 3 μg of MFL3 or the appropriate isotype antibody was injected into the left striatum of Vm/Dk mice. After 1 week, mice were sacrificed and the brains were extracted. Following immunohistochemical staining, GFP-positive cells in the contralateral hemisphere of three representative areas per sample were counted and normalized to the area of the tumor as assessed by Cell^R software (Olympus, Germany).

Migration Assay

Migration of the glioma cells in vitro was measured by the migration through Collagen I-coated (Chemicon) transwell inserts (Falcon). Cells (5×10^4) were plated in 200 μl medium onto collagen-coated (50 μg/ml) transwell inserts with 8 μm pore size. Twenty-four hours after plating, the cells were starved with basal DMEM for an additional 24 hr before they were treated with αApo-1 (1 μg/ml or 0.1 μg/ml + Protein-A for crosslinking), CD95L (10 ng/ml), and CD95L-T4 (20 ng/ml). The number of completely migrated cells was counted at 12, 24, and 48 hr after treatment. In every experiment triplicates were counted for each treatment.

Genetic Engineering of Human CD95-Ligand-T4

The TRAIL/DR5 complex and the TNF-α structure were used as models to develop expression strategies for the human CD95L-receptor binding domain (CD95L-RBD). Provided that the structure of trimeric human CD95L-RBD is in principle similar to the TNF-α or TRAIL-RBD structures (PDB entries: 1TNF and 1D0G/1DU3, respectively [Cha et al., 1999; Eck and Sprang, 1989; Hymowitz et al., 1999]), the following observations were taken into account:

(1) The N- and C-terminal amino acids of the RBD from TRAIL and TNF-α form an antiparallel β strand.
(2) The terminal amino acids of this β strand are located next to each other at the same site of the molecule close to the central axis of the TRAIL-RBD trimer (see Figure S1).

This means that, for steric reasons, the use of N and C termini in the same molecule for the fusion of protein domains (e.g., for the addition of stabilization motifs or tags) is mutually exclusive. The ideal stabilization motif should be a small, well-defined trimer located close to the central axis of the CD95L-trimer with its N and C terminus at opposite sites of the stabilization motif in order to minimize its risk of interference with the ligand/receptor interaction sites. An appropriate trimeric protein domain fulfilling these criteria is the T4-Foldon motif from the fibritin of the bacteriophage T4 (Guthe et al., 2004; Meier et al., 2004).

According to the above-mentioned considerations, the T4-Foldon was fused C-terminally to the human CD95L-RBD (Glu142-Leu281 of CD95L). Between the CD95L-RBD and the T4-Foldon, a flexible linker element (GSSGSSGSSGS) was placed, and a hexahistidine tag and a streptag-II (HHHHHHSAWSHPQFEK) were added C-terminally. This affinity tag was linked to the T4-Foldon by a flexible linker element (SGPSSSSS). To allow for secretory-based expression, a signal peptide from human Igκ was fused to the N terminus (Glu142). The proposed signal peptide cleavage site formed by the fusion of the Igκ leader to the CD95L-RBD is expected to release a final product with a N-terminal located Glutamine, corresponding to Glu142 of human CD95L. The amino acid sequence of the CD95L-T4-construct shown in Figure S1C was back-translated and its codon usage optimized for mammalian cell-based expression. Gene synthesis was done by ENTELECHON GmbH (Regensburg, Germany). The final expression cassette was subcloned into pCDNA4-HisMax-backbone, using unique HindIII and NotI sites of the plasmid. A schematic summary, including all features described above, is shown exemplarily for the TRAIL-T4-DR5-complex (Figure S1D).

Expression and Purification of CD95L-T4

HEK293T cells grown in DMEM + GlutaMAX (GibCo) supplemented with 10% FBS, 100 units/ml penicillin, and 100 μg/ml Streptomycin were transiently transfected with a plasmid encoding CD95L-T4. Cell culture supernatant containing recombinant CD95L-T4 was harvested 3 days posttransfection and clarified by centrifugation at 300 × g followed by filtration through a 0.22 μm sterile filter. For affinity purification, 1 ml Streptactin Sepharose (IBA GmbH, Göttingen, Germany) was packed to a column and equilibrated with 15 ml buffer W (100 mM Tris-HCl, 150 mM NaCl [pH 8.0]). The cell culture supernatant was applied to the column with a flow rate of 4 ml/min. Subsequently, the column was washed with buffer W, and bound CD95L-T4 was eluted stepwise by addition of 7 × 1 ml buffer E (100 mM Tris-HCl, 150 mM NaCl, 2.5 mM Desthiobiotin [pH 8.0]). The protein content of the eluate fractions was analyzed by SDS-PAGE and silver staining (Figure S1E). Fractions E2–E5 were subsequently concentrated by ultrafiltration and further analyzed by size exclusion chromatography (SEC).

SEC was performed on a Superdex 200 column using an Äkta chromatography system (GE-Healthcare). The column was equilibrated with phosphate-buffered saline, and the concentrated, streptactin-purified CD95L-T4 (E2-E5) was loaded onto the SEC column at a flow rate of 0.5 ml/min. The elution of CD95L-T4 was monitored by absorbance at 280 nm. The apparent molecular weight of purified CD95L-T4 was determined based on calibration of the Superdex 200 column with gel filtration standard proteins (Figures S1F and S1G) (Bio-Rad GmbH, München, Germany).

SUPPLEMENTAL DATA

The Supplemental Data include Supplemental Experimental Procedures and three supplemental figures and can be found with this article online at http://www.cancercell.org/cgi/content/full/13/3/235/DC1/.

ACKNOWLEDGMENTS

We thank Hilde Discher and Stefanie Krauth for valuable technical support and Jochen Hess for help with Zymography assay. We also thank Bernhard Radlwimmer for the CGH-analysis of NCH cells. We thank Dr. Min Li-Weber for the NFκB-luciferase reporter construct and Prof. Peter H. Krammer for the agonistic antibody to CD95. We thank Prof. Otmar D. Wiestler for critical reading of the manuscript. This work was supported by the German Research Foundation (DFG), the German Federal Ministry of Education and Research (BMBF), and the Paul Ehrlich Foundation.

Received: June 12, 2007
Revised: November 20, 2007
Accepted: February 5, 2008
Published: March 10, 2008

REFERENCES

Ashley, D.M., Kong, F.M., Bigner, D.D., and Hale, L.P. (1998). Endogenous expression of transforming growth factor beta1 inhibits growth and tumorigenicity and enhances Fas-mediated apoptosis in a murine high-grade glioma model. Cancer Res. *58*, 302–309.

Barnhart, B.C., Legembre, P., Pietras, E., Bubici, C., Franzoso, G., and Peter, M.E. (2004). CD95 ligand induces motility and invasiveness of apoptosis-resistant tumor cells. EMBO J. *23*, 3175–3185.

Biancone, L., Martino, A.D., Orlandi, V., Conaldi, P.G., Toniolo, A., and Camussi, G. (1997). Development of inflammatory angiogenesis by local stimulation of Fas in vivo. J. Exp. Med. *186*, 147–152.

Boggon, T.J., and Eck, M.J. (2004). Structure and regulation of Src family kinases. Oncogene *23*, 7918–7927.

Boldin, M.P., Varfolomeev, E.E., Pancer, Z., Mett, I.L., Camonis, J.H., and Wallach, D. (1995). A novel protein that interacts with the death domain of Fas/APO1 contains a sequence motif related to the death domain. J. Biol. Chem. *270*, 7795–7798.

Cha, S.S., Shin, H.C., Choi, K.Y., and Oh, B.H. (1999). Expression, purification and crystallization of recombinant human TRAIL. Acta Crystallogr. D Biol. Crystallogr. *55*, 1101–1104.

Choi, C., Xu, X., Oh, J.W., Lee, S.J., Gillespie, G.Y., Park, H., Jo, H., and Benveniste, E.N. (2001). Fas-induced expression of chemokines in human glioma cells: Involvement of extracellular signal-regulated kinase 1/2 and p38 mitogen-activated protein kinase. Cancer Res. *61*, 3084–3091.

Choi, C., Gillespie, G.Y., Van Wagoner, N.J., and Benveniste, E.N. (2002). Fas engagement increases expression of interleukin-6 in human glioma cells. J. Neurooncol. *56*, 13–19.

Choi, K., Benveniste, E.N., and Choi, C. (2003). Induction of intercellular adhesion molecule-1 by Fas ligation: Proinflammatory roles of Fas in human astroglioma cells. Neurosci. Lett. *352*, 21–24.

Cursi, S., Rufini, A., Stagni, V., Condo, I., Matafora, V., Bachi, A., Bonifazi, A.P., Coppola, L., Superti-Furga, G., Testi, R., and Barila, D. (2006). Src kinase phosphorylates Caspase-8 on Tyr380: A novel mechanism of apoptosis suppression. EMBO J. *25*, 1895–1905.

Daigle, I., Yousefi, S., Colonna, M., Green, D.R., and Simon, H.U. (2002). Death receptors bind SHP-1 and block cytokine-induced anti-apoptotic signaling in neutrophils. Nat. Med. *8*, 61–67.

Demjen, D., Klussmann, S., Kleber, S., Zuliani, C., Stieltjes, B., Metzger, C., Hirt, U.A., Walczak, H., Falk, W., Essig, M., et al. (2004). Neutralization of CD95 ligand promotes regeneration and functional recovery after spinal cord injury. Nat. Med. *10*, 389–395.

Eastman, Q., and Grosschedl, R. (1999). Regulation of LEF-1/TCF transcription factors by Wnt and other signals. Curr. Opin. Cell Biol. *11*, 233–240.

Eberle, A., Reinehr, R., Becker, S., and Haussinger, D. (2005). Fluorescence resonance energy transfer analysis of proapoptotic CD95-EGF receptor interactions in Huh7 cells. Hepatology *41*, 315–326.

Eck, M.J., and Sprang, S.R. (1989). The structure of tumor necrosis factor-alpha at 2.6 A resolution. Implications for receptor binding. J. Biol. Chem. *264*, 17595–17605.

Eischen, C.M., Dick, C.J., and Leibson, P.J. (1994). Tyrosine kinase activation provides an early and requisite signal for Fas-induced apoptosis. J. Immunol. *153*, 1947–1954.

Fan, X., Aalto, Y., Sanko, S.G., Knuutila, S., Klatzmann, D., and Castresana, J.S. (2002). Genetic profile, PTEN mutation and therapeutic role of PTEN in glioblastomas. Int. J. Oncol. *21*, 1141–1150.

Frei, K., Ambar, B., Adachi, N., Yonekawa, Y., and Fontana, A. (1998). Ex vivo malignant glioma cells are sensitive to Fas (CD95/APO-1) ligand-mediated apoptosis. J. Neuroimmunol. *87*, 105–113.

Furnari, F.B., Lin, H., Huang, H.S., and Cavenee, W.K. (1997). Growth suppression of glioma cells by PTEN requires a functional phosphatase catalytic domain. Proc. Natl. Acad. Sci. USA *94*, 12479–12484.

Gulbins, E., Hermisson, M., Brenner, B., Grassme, H.U., Linderkamp, O., Dichgans, J., Weller, M., and Lang, F. (1998). Cellular stimulation via CD95 involves activation of phospho-inositide-3-kinase. Pflugers Arch. *435*, 546–554.

Gum, R., Lengyel, E., Juarez, J., Chen, J.H., Sato, H., Seiki, M., and Boyd, D. (1996). Stimulation of 92-kDa gelatinase B promoter activity by ras is mitogen-activated protein kinase kinase 1-independent and requires multiple transcription factor binding sites including closely spaced PEA3/ets and AP-1 sequences. J. Biol. Chem. *271*, 10672–10680.

Guthe, S., Kapinos, L., Moglich, A., Meier, S., Grzesiek, S., and Kiefhaber, T. (2004). Very fast folding and association of a trimerization domain from bacteriophage T4 fibritin. J. Mol. Biol. *337*, 905–915.

Hohlbaum, A.M., Saff, R.R., and Marshak-Rothstein, A. (2002). Fas-ligand—Iron fist or Achilles' heel? Clin. Immunol. *103*, 1–6.

Hymowitz, S.G., Christinger, H.W., Fuh, G., Ultsch, M., O'Connell, M., Kelley, R.F., Ashkenazi, A., and de Vos, A.M. (1999). Triggering cell death: The crystal structure of Apo2L/TRAIL in a complex with death receptor 5. Mol. Cell *4*, 563–571.

Jarad, G., Wang, B., Khan, S., DeVore, J., Miao, H., Wu, K., Nishimura, S.L., Wible, B.A., Konieczkowski, M., Sedor, J.R., and Schelling, J.R. (2002). Fas activation induces renal tubular epithelial cell beta 8 integrin expression and function in the absence of apoptosis. J. Biol. Chem. *277*, 47826–47833.

Karmakar, S., Weinberg, M.S., Banik, N.L., Patel, S.J., and Ray, S.K. (2006). Activation of multiple molecular mechanisms for apoptosis in human malignant glioblastoma T98G and U87MG cells treated with sulforaphane. Neuroscience *141*, 1265–1280.

Kischkel, F.C., Hellbardt, S., Behrmann, I., Germer, M., Pawlita, M., Krammer, P.H., and Peter, M.E. (1995). Cytotoxicity-dependent APO-1 (Fas/CD95)-associated proteins form a death-inducing signaling complex (Dros. Inf. Serv.C) with the receptor. EMBO J. *14*, 5579–5588.

Kischkel, F.C., Lawrence, D.A., Tinel, A., LeBlanc, H., Virmani, A., Schow, P., Gazdar, A., Blenis, J., Arnott, D., and Ashkenazi, A. (2001). Death receptor recruitment of endogenous caspase-10 and apoptosis initiation in the absence of caspase-8. J. Biol. Chem. *276*, 46639–46646.

Kleihues, P., Burger, P.C., and Scheithauer, B.W. (1993). The new WHO classification of brain tumours. Brain Pathol. *3*, 255–268.

Krammer, P.H. (2000). CD95's deadly mission in the immune system. Nature *407*, 789–795.

Kugler, W., Erdlenbruch, B., Junemann, A., Heinemann, D., Eibl, H., and Lakomek, M. (2002). Erucylphosphocholine-induced apoptosis in glioma cells: Involvement of death receptor signalling and caspase activation. J. Neurochem. *82*, 1160–1170.

Lee, J.K., Sayers, T.J., Back, T.C., Wigginton, J.M., and Wiltrout, R.H. (2003). Lack of FasL-mediated killing leads to in vivo tumor promotion in mouse Lewis lung cancer. Apoptosis *8*, 151–160.

Madrid, L.V., Wang, C.Y., Guttridge, D.C., Schottelius, A.J., Baldwin, A.S., Jr., and Mayo, M.W. (2000). Akt suppresses apoptosis by stimulating the transactivation potential of the RelA/p65 subunit of NF-κB. Mol. Cell. Biol. *20*, 1626–1638.

Mann, B., Gelos, M., Siedow, A., Hanski, M.L., Gratchev, A., Ilyas, M., Bodmer, W.F., Moyer, M.P., Riecken, E.O., Buhr, H.J., and Hanski, C. (1999). Target genes of beta-catenin-T cell-factor/lymphoid-enhancer-factor signaling in human colorectal carcinomas. Proc. Natl. Acad. Sci. USA *96*, 1603–1608.

Martin-Villalba, A., Herr, I., Jeremias, I., Hahne, M., Brandt, R., Vogel, J., Schenkel, J., Herdegen, T., and Debatin, K.M. (1999). CD95 ligand (Fas-L/APO-1L) and tumor necrosis factor-related apoptosis- inducing ligand mediate ischemia-induced apoptosis in neurons. J. Neurosci. *19*, 3809–3817.

Martin-Villalba, A., Hahne, M., Kleber, S., Vogel, J., Falk, W., Schenkel, J., and Krammer, P.H. (2001). Therapeutic neutralization of CD95L and TNF attenuates brain damage in stroke. Cell Death Differ. *8*, 679–686.

Mattson, M.P. (2000). Apoptosis in neurodegenerative disorders. Nat. Rev. Mol. Cell Biol. *1*, 120–129.

Medema, J.P., Scaffidi, C., Kischkel, F.C., Shevchenko, A., Mann, M., Krammer, P.H., and Peter, M.E. (1997). FLICE is activated by association with the CD95 death-inducing signaling complex (Dros. Inf. Serv.C). EMBO J. *16*, 2794–2804.

Meier, S., Guthe, S., Kiefhaber, T., and Grzesiek, S. (2004). Foldon, the natural trimerization domain of T4 fibritin, dissociates into a monomeric A-state form containing a stable beta-hairpin: Atomic details of trimer dissociation and local beta-hairpin stability from residual dipolar couplings. J. Mol. Biol. *344*, 1051–1069.

Ozes, O.N., Mayo, L.D., Gustin, J.A., Pfeffer, S.R., Pfeffer, L.M., and Donner, D.B. (1999). NF-κB activation by tumour necrosis factor requires the Akt serine-threonine kinase. Nature *401*, 82–85.

Park, C.M., Park, M.J., Kwak, H.J., Lee, H.C., Kim, M.S., Lee, S.H., Park, I.C., Rhee, C.H., and Hong, S.I. (2006). Ionizing radiation enhances matrix metalloproteinase-2 secretion and invasion of glioma cells through Src/Epidermal Growth Factor Receptor-mediated p38/Akt and Phosphatidylinositol 3-Kinase/Akt signaling pathways. Cancer Res. *66*, 8511–8519.

Rao, J.S. (2003). Molecular mechanisms of glioma invasiveness: The role of proteases. Nat. Rev. Cancer *3*, 489–501.

Reya, T., and Clevers, H. (2005). Wnt signalling in stem cells and cancer. Nature *434*, 843–850.

Sato, H., and Seiki, M. (1993). Regulatory mechanism of 92 kDa type IV collagenase gene expression which is associated with invasiveness of tumor cells. Oncogene *8*, 395–405.

Sawaya, R., Go, Y., Kyritisis, A.P., Uhm, J., Venkaiah, B., Mohanam, S., Gokaslan, Z.L., and Rao, J.S. (1998). Elevated levels of Mr 92,000 type IV collagenase during tumor growth in vivo. Biochem. Biophys. Res. Commun. *251*, 632–636.

Scaffidi, C., Fulda, S., Srinivasan, A., Friesen, C., Li, F., Tomaselli, K.J., Debatin, K.M., Krammer, P.H., and Peter, M.E. (1998). Two CD95 (APO-1/Fas) signaling pathways. EMBO J. *17*, 1675–1687.

Schlottmann, K.E., Gulbins, E., Lau, S.M., and Coggeshall, K.M. (1996). Activation of Src-family tyrosine kinases during Fas-induced apoptosis. J. Leukoc. Biol. *60*, 546–554.

Shinohara, H., Yagita, H., Ikawa, Y., and Oyaizu, N. (2000). Fas drives cell cycle progression in glioma cells via extracellular signal-regulated kinase activation. Cancer Res. *60*, 1766–1772.

Staal, F.J., Weerkamp, F., Baert, M.R., van den Burg, C.M., van Noort, M., de Haas, E.F., and van Dongen, J.J. (2004). Wnt target genes identified by DNA microarrays in immature CD34+ thymocytes regulate proliferation and cell adhesion. J. Immunol. *172*, 1099–1108.

Stirnweiss, J., Valkova, C., Ziesche, E., Drube, S., and Liebmann, C. (2006). Muscarinic M2 receptors mediate transactivation of EGF receptor through Fyn kinase and without matrix metalloproteases. Cell. Signal. *18*, 1338–1349.

Thomas, S.M., and Brugge, J.S. (1997). Cellular functions regulated by Src family kinases. Annu. Rev. Cell Dev. Biol. *13*, 513–609.

Troussard, A.A., Costello, P., Yoganathan, T.N., Kumagai, S., Roskelley, C.D., and Dedhar, S. (2000). The integrin linked kinase (ILK) induces an invasive phenotype via AP-1 transcription factor-dependent upregulation of matrix metalloproteinase 9 (MMP-9). Oncogene *19*, 5444–5452.

Valente, P., Fassina, G., Melchiori, A., Masiello, L., Cilli, M., Vacca, A., Onisto, M., Santi, L., Stetler-Stevenson, W.G., and Albini, A. (1998). TIMP-2 overexpression reduces invasion and angiogenesis and protects B16F10 melanoma cells from apoptosis. Int. J. Cancer *75*, 246–253.

Weller, M., Frei, K., Groscurth, P., Krammer, P.H., Yonekawa, Y., and Fontana, A. (1994). Anti-Fas/APO-1 antibody-mediated apoptosis of cultured human glioma cells. Induction and modulation of sensitivity by cytokines. J. Clin. Invest. *94*, 954–964.

Wong, B.R., Besser, D., Kim, N., Arron, J.R., Vologodskaia, M., Hanafusa, H., and Choi, Y. (1999). TRANCE, a TNF family member, activates Akt/PKB through a signaling complex involving TRAF6 and c-Src. Mol. Cell *4*, 1041–1049.

Zuliani, C., Kleber, S., Klussmann, S., Wenger, T., Kenzelmann, M., Schreglmann, N., Martinez, A., del Rio, J.A., Soriano, E., Vodrazka, P., et al. (2006). Control of neuronal branching by the death receptor CD95 (Fas/Apo-1). Cell Death Differ. *13*, 31–40.